A Scanning Tunneling Microscopy Study of Electrostatic and Proximity Effects in Tip-Assisted Migration and Desorption of a DNA Base Molecule on $SrTiO_3$

Ryota Akiyama,† Takuya Matsumoto,‡ and Tomoji Kawai*

The Institute of Scientific and Industrial Research, Osaka University, 8-1 Mihogaoka, Ibaraki, Osaka 567-0047, Japan

Received: November 23, 1998

Manipulation of DNA base molecules has been achieved using the tip of a scanning tunneling microscope (STM). The authors have identified three distinct manipulation modes, namely, lateral sliding by proximity effect and migration and extraction by electrostatic forces for adenine (one of the DNA base molecules) on the $SrTiO_3(100)$-$\sqrt{5}\times\sqrt{5}$ surface. The mechanisms of these modes have been revealed by measuring the absolute separation between the tip and the surface (or the adsorbate) from the current versus tip displacement relationship, and the surface dipole moment using tunneling barrier height measurement. Controlling the tip−surface separation has revealed that the proximity effect can be attributed to the chemical forces acting with a critical tip−surface internuclear separation of 4.4 Å. Conversely, the extraction and sliding induced by electrostatic interaction show striking bias polarity dependence. This behavior is determined by the electrostatic stability of the surface dipole under the tip field.

1. Introduction

The scanning tunneling microscope (STM) has been employed in attempts to manipulate adsorbates on a subnanometer scale. This STM manipulation represents a significant contribution to the advancement of nanometer-order physics, by permitting the construction of atomic-level artificial structures on the surfaces. Recently, STM manipulation has even had an impact in chemistry and biology. Interest in the manipulation of organic molecules has grown in the areas of molecular devices, individually controlled chemical reactions, and biophysics. To support such requirements, improved methods of controlling molecular manipulation must be developed. Since the electronic properties of molecules are largely determined by the molecular structures involved, characteristic mechanisms for molecular manipulation are expected.

Reports have been already published for the molecular manipulation of large molecules such as Cu-TBP-porphyrin,[1] C_{60},[2] and DNA oligomer,[3] which are positioned individually by the tip pushing laterally. This lateral pushing mechanism is suitable for structurally high molecules on the surfaces. However, if this pushing mechanism is applied to structurally low molecules, extremely high stability is required to prevent both the tip damaging the molecule and the surface. Conversely, electronic excitations occurring within a strong electric field offer superior features, specifically the possibility of the contact-free positioning of small adsorbate. In these cases, adsorbate extraction has been explained by a field evaporation process[4−13] or an electronic/vibrational excitation process.[16,17] The lateral sliding of the adsorbate has been accepted as an electrostatic interaction between the dipole moment and an electric field.[10−15] The individual manipulation mechanisms are supported by theoretical studies, although quantitative analysis and generalized interpretation have not been undertaken to date.

From a practical point of view, the kind of substrate is crucial for the manipulation of small molecules at room temperature. The tip-assisted movement of individual molecules requires appropriate bonding between an isolated molecule and a surface in the range of the adsorption energy in order to prevent thermal diffusion and to permit tip-induced migration without breaking intramolecular bonds. For small molecules such as nucleic acid bases, however, it is difficult to satisfy the criteria for manipulation on the surface of conventional substrates at room temperature. For example, adenine molecules on the Cu(111) surface migrate easily due to thermal diffusion and form self-assembled structures at room temperature.[18,19] On the other hand, adenine on the Pd(110) surface and Si(100)-2×1 surface cannot be moved by the tip because of their strong binding energy between adenine molecules and the surface.[20−22]

This report describes the authors' achievement of tip-assisted lateral sliding, migration, and desorption of adenine molecules (one of the DNA base molecules) on an $SrTiO_3(100)$-$\sqrt{5}\times\sqrt{5}$ surface. The $SrTiO_3(100)$-$\sqrt{5}\times\sqrt{5}$ surface has small corrugation and a moderate binding energy to adenine molecules compared with other conventional substrates. This system shows a variety of manipulation modes occurring selectively depending upon the tip−surface separation, the electric field, and the electric dipole moment. Quantitative measurements and analysis reveal two types of manipulation mode: the proximity effect and field−dipole interaction. In the former mode, the manipulation occurs in the near-contact region, which is clearly distinct from the pushing mechanism. Conversely, the electrostatic interaction between the electric field and dipole moment arising at the surface molecule is significant in the latter case.

2. Experimental Section

(a) Equipment. All the STM-imaging and manipulation experiments were performed using a USM-301 manufactured

* Corresponding author. Phone: 81-6-6879-8445. FAX: 81-6-6875-2440. E-mail: kawai@sanken.osaka-u.ac.jp.

† Phone: 81-6-6879-8446. FAX: 81-6-6875-2440. E-mail: akkin32@sanken.osaka-u.ac.jp.

‡ Phone: 81-6-6879-8524. FAX: 81-6-6875-2440. E-mail: matsumoto@sanken.osaka-u.ac.jp.

10.1021/jp984519h CCC: $18.00
Published on Web 07/03/1999

by UNISOKU (of Osaka, Japan). The *XYZ* scale was calibrated by imaging a commonly used Si(111)-7×7 surface. The experiments were conducted in an ultrahigh vacuum (UHV) chamber with a base pressure of 8.0×10^{-11} Torr. The STM chamber was equipped with a preparation chamber for sample heating and various surface treatments, whose base pressure is 5.0×10^{-9} Torr. Mechanically formed PtIr tips were used for all experiments described in this report.

(b) Sample Preparation. The $SrTiO_3(100)$-$\sqrt{5}\times\sqrt{5}$ surface used as substrates for depositing adenine molecules was prepared using the following procedure.[23] A polished and (100)-oriented plate-shaped $SrTiO_3$ crystal was purchased from Earth Chemical Co. (of Osaka, Japan). The crystal was clamped on an Si heater mounted on a holder made of Ta and Mo. The sample was preheated for degassing at 600 °C for 3 h in the preparation chamber and further annealed at 1185 ± 5 °C for 2 min in the main chamber. The sample temperature was measured using an optical pyrometer. The chamber pressure during annealing did not exceed 1.0×10^{-9} Torr. After annealing, the sample was transferred to the STM head, and an atomic resolution of the surface was able to be obtained within 2 h.

The adenine molecule powder was placed in small deposition cell made of Ta foil and introduced into the preparation chamber. Prior to the deposition, the deposition cell was preheated for degassing at 120 °C for 1 h while being monitored by a quadrupole mass filter. The adenine molecule was deposited on the $\sqrt{5}\times\sqrt{5}$ surface by heating the cell to 200 °C.

(c) Molecular Manipulation. The tip-assisted manipulation of the adenine molecules was achieved as follows. First, an STM image of a large area was obtained with a tunneling current of 7−10 pA and a sample bias voltage of −2 V. Tip-assisted manipulation was then induced by tip-scanning over the molecules with a varying sample bias (with a fixed tunneling current of 10 pA) or a varying image tunneling current (with a fixed sample bias of ±2 V) in a closed feedback loop. Finally, a new STM image of the identical area was scanned to check the manipulation result.

(d) log(*I*)−Δ*z* Spectroscopy. The absolute tip−sample separation *z* under the various feedback conditions of tunneling current and bias voltage were estimated using the following procedures.[11] As the first step, the authors measured tip-displacement Δ*z* from the reference probe position z_{ref} to the contact position against the surface. The contact position was defined as a "current jump", indicating the change from vacuum electron tunneling to conductive current.[24−28] In the actual measurement of $I(\Delta z)$, the dynamic range of the current amplifier was limited when the tip was scanned along the *z*-direction over the full tip-displacement range. For this reason, the values of $I(\Delta z)$ were measured as a partial data series obtained at different feedback positions with tunneling currents *I* of 7, 70, 700, and 7000 pA and a displacement Δ*z* of ±3 Å. Overall characteristics were then built up to overlap the data following measurement. All $I(\Delta z)$ measurements were performed during the open feedback loop for 1.3 s.

For the second step, the authors measured values of Δ*z* from the reference tip position z_{ref} for various combinations of *I* and V_s under closed feedback operation. The Δ*z* values were influenced by the electronic properties of the surface, as discussed later.

Generally, an electrical atomic contact is regarded as a bond between two atoms. In such a case, the internuclear separation *z*′ can be defined as the bond length. Conversely, an electric field *F* between the tip atom and the surface atom should be defined using the separation between their rigid sphere surfaces

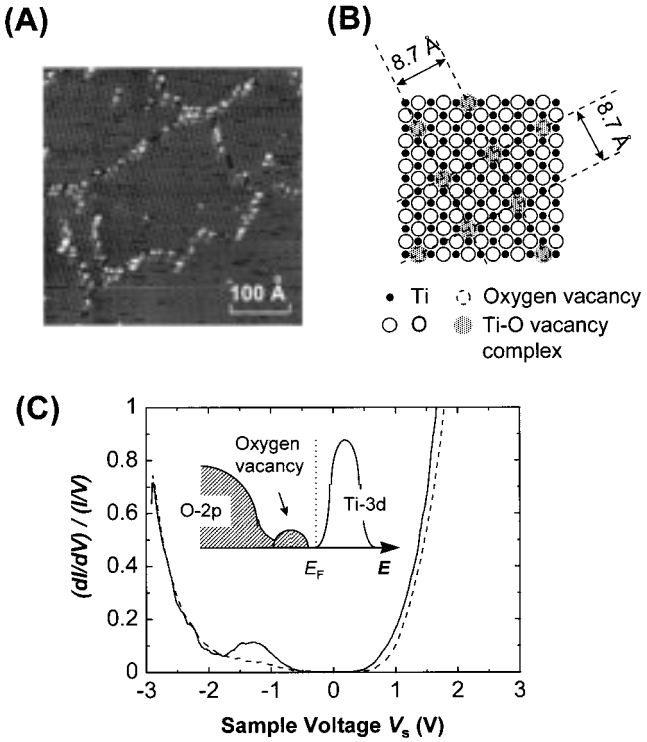

Figure 1. (A) Constant-current STM image of the $SrTiO_3(100)$-$\sqrt{5}\times\sqrt{5}$ surface taken with $V_s = -2$ V and $I = 7$ pA. (B) Model of the $SrTiO_3(100)$-$\sqrt{5}\times\sqrt{5}$ reconstructed surface that has TiO_2 vacancy complexes ordering in $\sqrt{5}\times\sqrt{5}$ in the TiO_2 top layer. (C) Normalized conductance of the $SrTiO_3(100)$-$\sqrt{5}\times\sqrt{5}$ surface referred to in ref 23. The solid and dotted lines represent the spectra at the ordered bright TiO_2 vacancy spots and in the dark region in the STM images, respectively.

z with a radius of $r_F = 1/k_F$, where k_F is the Fermi wavenumber. Consequently, the relationship between these separations can be expressed as

$$z = z' - 2r_F \tag{1}$$

For this research, the authors used the value of platinum for r_F, 0.72 Å, and electrical contact therefore occurred at $z = 0$ A ($z' = 1.44$ Å). The electric field was given by $F = V_s/z$.

(e) Imaging of Tunneling Barrier Height. On the basis of a simple one-dimensional tunneling model, the tunneling barrier-height Φ has been generally defined as

$$\Phi = -0.952[\Delta \ln(I)/\Delta z\,]^2 \tag{2}$$

where *I* is the tunneling current and *z* is the tip−surface separation.[25−28] As a corresponding experiment, a lock-in technique was used to measure $\Delta\ln(I)$ with a modulating tip−surface displacement Δ*z*.[29] The modulation amplitude, frequency, and time constant were $\Delta z = 1$ Å, $f = 4$ kHz, and $\tau = 3$ ms, respectively. In the actual scan for barrier height imaging, the protrusions in the molecular image accompanied a bunching caused by a transient response of electronics. Therefore, such components were carefully removed in order to estimate the absolute value of the tunneling barrier height.

3. Adenine Molecules on $SrTiO_3(100)$-$\sqrt{5}\times\sqrt{5}$ Surfaces

(a) $SrTiO_3(100)$-$\sqrt{5}\times\sqrt{5}$ Surface. The structure and electronic properties of a $SrTiO_3(100)$-$\sqrt{5}\times\sqrt{5}$ surface are shown in Figure 1. An atomic-scale image of a 440 × 440 Å^2 region of a $\sqrt{5}\times\sqrt{5}$ surface is shown in Figure 1A. The bright spots

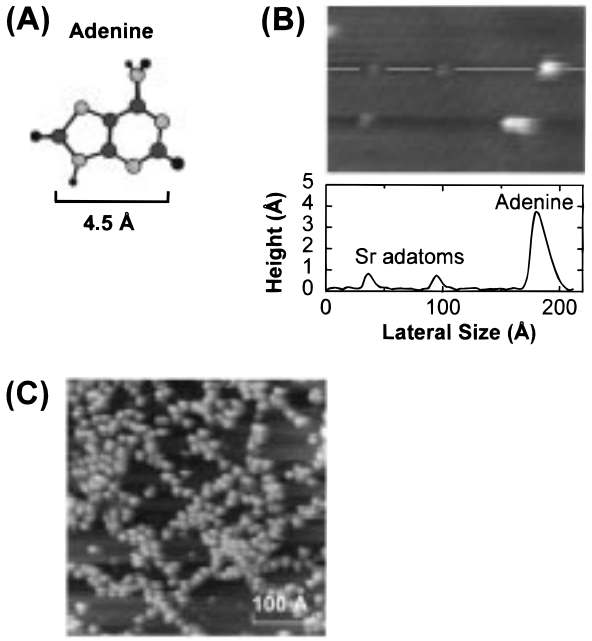

Figure 2. (A) Adenine molecule structure. (B) Constant-current STM image and cross-sectional profile of adenine molecules deposited on a $SrTiO_3(100)$-$\sqrt{5}\times\sqrt{5}$ surface with $V_s = -2$ V and $I = 7$ pA. The Sr adatom and adenine molecule can be distinguished by their heights. (C) Constant-current STM image of adenine molecules with high coverage on the $SrTiO_3(100)$-$\sqrt{5}\times\sqrt{5}$ surface ($I = 7$ pA and $V_s = -2.0$ V).

are ordered as square lattices, resulting from the ordering of the Ti−O vacancy complexes in the $\sqrt{5}\times\sqrt{5}$-R±26.6° superstructures, as shown in Figure 1B. The subatomic corrugation is approximately 0.2 Å, similar to previous observations on metal surfaces. The surface is divided by rotational and phase-shifted domain boundaries. A number of Sr atoms located on these domain boundaries appear as bright protrusions. Only a few Sr atoms are also found inside the domains.

Figure 1C shows tunneling spectra measured at the two types of locations on the $\sqrt{5}\times\sqrt{5}$ structure.[23] The solid line indicates the ordered bright spots corresponding to Ti−O vacancy, and the dashed line indicates the dark regions in the STM images. The dark region spectrum indicates an energy gap of about 3 eV, which agrees with the band-gap value for stoichiometric $SrTiO_3$. Conversely, the bright region revealed localized states at $E = -1.35$ eV below the Fermi level. This corresponds to an oxygen vacancy state appearing inside the band gap previously reported in photoemission experiments and in DV-Xα calculations. The work function of the $SrTiO_3(100)$-$\sqrt{5}\times\sqrt{5}$ surface is $\phi = 4.2$ eV, which has been obtained from photoemission studies.[30]

(b) Adsorption Structure of the Adenine Molecule. The adenine molecule is one of the nucleic acid bases (DNA base molecules), which has two conjugated rings, as shown in Figure 2A. After the deposition of this molecule on the $SrTiO_3(100)$-$\sqrt{5}\times\sqrt{5}$ surface, large and round protrusions appear, as shown in Figure 2B. We confirm that these round protrusions are adenine molecules because they increase in number with increasing deposition time. The STM images of adenine molecules and Sr atoms are easily distinguished by their height and lateral size, as shown in the cross sectional profile in Figure 2B. The heights and lateral size of the image of adenine molecules are 3−4 and 10−20 Å, whereas those of Sr atoms are approximately 1 and 6−10 Å, respectively.[31] With a high coverage of adenine molecules on the $\sqrt{5}\times\sqrt{5}$ surface, as shown in Figure 2C, most of the adenine molecules were trapped in the domain boundaries and only a few in the domains. This indicates that adenine molecules cannot be fixed intrinsically on a clean terrace of an $SrTiO_3(100)$-$\sqrt{5}\times\sqrt{5}$ surface at room temperature if no anchor sites such as Sr atoms exist at surface boundaries or defects.

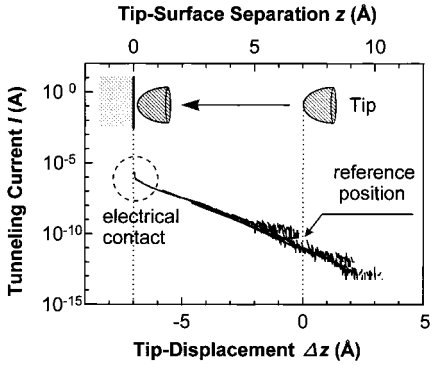

Figure 3. Typical relationship between tunneling current I and tip-displacement Δz, measured for various feedback positions ($V_s = -2$ V and $I = 7$, 70, 700, 7000 pA). The contact between the tip and the surface ($z = 0$) was defined by current jump, specifically the change from tunneling current to conductive current. The reference probe position z_{ref} was then calibrated for $z_{ref} = 7$ Å ($z' \cong 8.4$ Å), as shown in the upper scale.

4. Molecular Manipulation

(a) Tip−Surface Separation and Electric Field. In manipulation experiments, the tip−surface separation z is a significant parameter because it directly influences the electric field strength and the atomic forces acting between the tip and the adsorbate/surface. Accordingly, absolute tip−surface separation z for various combinations of I and V_s were predetermined as follows.[11]

Figure 3 shows typical plots of tunneling current I against tip-displacement Δz for determining the reference feedback position z_{ref} (z'_{ref}) ($I = 7$ pA and $V_s = -2$ V). The $I(\Delta z)$ curves were obtained at a series of different feedback positions controlled by the feedback current and then superimposed. The $I(\Delta z)$ curves overlap on a single line despite involving quite different feedback positions. When the tip approaches the surface from a reference feedback position, the logarithm of tunneling current, $\log I(\Delta z)$, increases linearly following a one-dimensional tunneling model. This is a typical result for metal surfaces studied in previous research.[24−28] When the tip reaches $\Delta z = -7$ Å, the curves show a steep "current jump", indicating a change from vacuum tunneling to conductive current. This can be explained by an electrical contact forming between the tip atoms and the surface atoms. As a result, z_{ref} (z'_{ref}) for a filled state ($I = 7$ pA and $V_s = -2$ V) was calibrated for $z = 7$ Å ($z' = 8.4$ Å), as shown on the upper scale in Figure 2. Similarly, z_{ref} for an empty state ($I = 7$ pA and $V_s = 2$ V) can be determined as $z = 13.5$ Å ($z' = 14.9$ Å) (not shown here). The distribution of the z_{ref} (z'_{ref}) values determined in this way depends on the tip conditions. Consequently, z_{ref} was measured many times, and the most reliable value was then used for the absolute tip−surface separation.

Using the reference tip positions z_{ref} (z'_{ref}), determined above, the variation of z (z') and F values was plotted as a function of I, as shown in Figure 4A. In the empty state ($V_s = 2$ V, solid circles), the tip approaches from $z = 13.5$ Å ($z' = 14.9$ Å) in 2.0-Å steps with the value of I increasing by 1 order of magnitude. In the same manner, the tip approaches in 1.2 Å

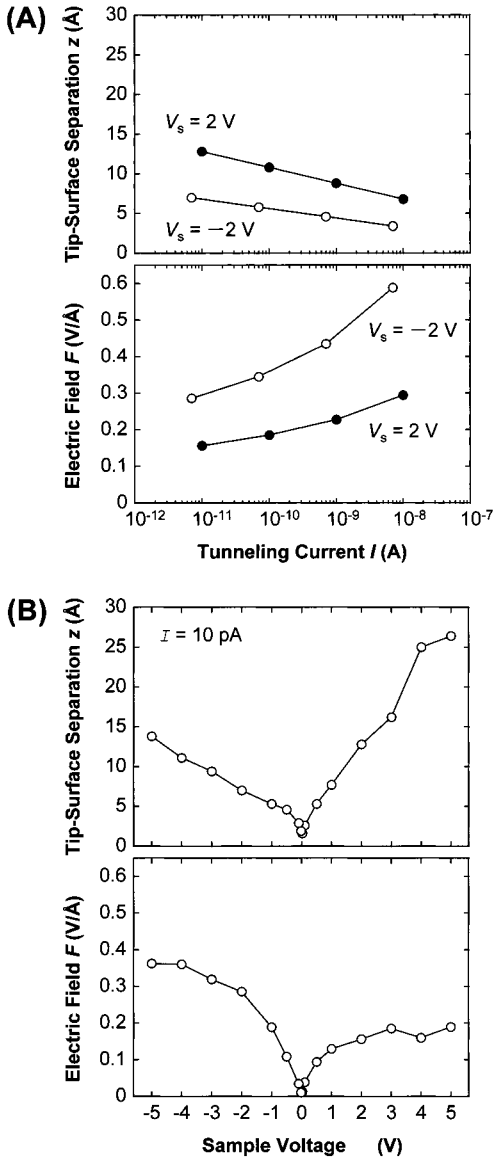

Figure 4. (A) Changes in tip−surface separation z (upper) and electric field F (lower) in terms of tunneling current I. The solid and hollow circles are measured at the empty state ($V_s = 2$ V) and filled state ($V_s = -2$ V), respectively. (B) Changes in tip−surface separation z (upper) and electric field F (lower) in terms of bias voltage V_s. These are measured at $I = 7-10$ pA.

steps from $z = 7$ Å ($z' = 8.4$ Å) in a filled state ($V_s = -2$ V, hollow circles). This linear relationship has already been discussed in Figure 3. The difference between the tip−surface separations z at filled and empty states can be interpreted by the band structure of the $\sqrt{5}\times\sqrt{5}$ surface as shown in Figure 1C. In the empty states, the density of states (DOS) of the Ti-3d orbital lie just above the Fermi level. Accordingly, the tip−surface separation for empty states is larger than that for filled states under the same feedback conditions.

Conversely, Figure 4B shows how z and F vary with V_s. With increasing bias voltage in both bias polarities, the tip retracts further from the surface in an empty state than in a filled state. Furthermore, when V_s is reduced to nearly 0 V, the tip approaches the surface very rapidly. This behavior is characteristic of a $\sqrt{5}\times\sqrt{5}$ surface band structure, which differs markedly from that of conventional metal surfaces. The electronic structure of reduced $SrTiO_3$ can be basically described as an electron-doped rigid-band semiconductor with a band gap of 3 eV, as shown in Figure 1C. The Fermi level is located at the edge of the Ti-3d conduction band, and DOS at the Fermi level is extremely small compared with conventional metal surfaces. For this reason, the bias dependencies of F and z are steep for an empty state and slow for a filled state. F becomes saturated around 0.36 and 0.2 V/Å for filled and empty states, respectively. Furthermore, for a low bias voltage, the tip approaches extremely close to the surface in order to obtain a tunneling current.

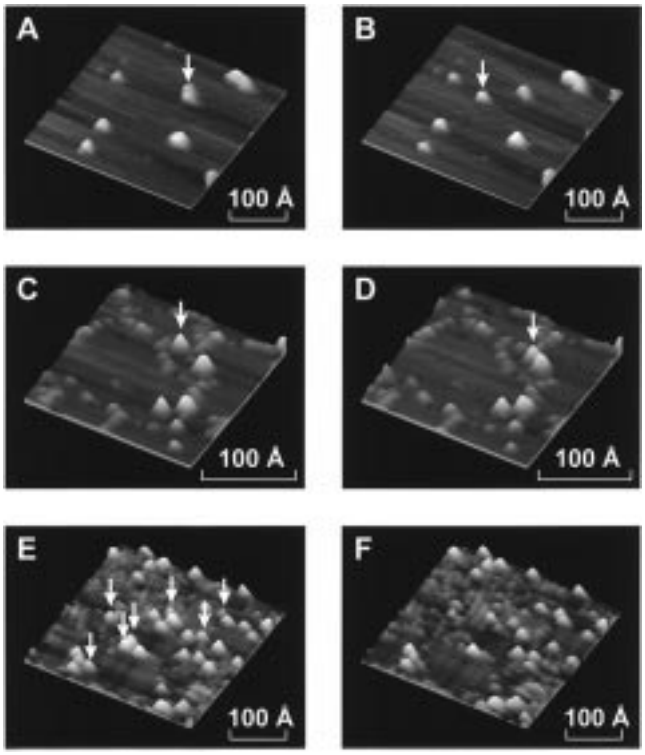

Figure 5. Movement of adenine molecules. With a negative sample voltage ($V_s = -2$ V), the STM images indicate the surface migration in (A) before and (B) after scanning with a large tunneling current $I =$ 700 pA (300 × 300 Å^2). The tip-assisted migration is also observed with a low voltage $I = 70$ pA and $V_s = -0.02$ V, as shown in (C) and (D) (180 × 180 Å^2). In contrast, with a positive sample voltage, the adenine molecules observed in the STM image shown in (E) disappeared from the surface after a high-voltage scan with $V_s = 4$ V and $I = 10$ pA, as shown in (F), suggesting desorption of the adenine molecule (300 × 300 Å^2).

(b) Tip-Assisted Migration and Desorption. The tip-assisted migration and desorption of adenine molecules on the $SrTiO_3$-(100)-$\sqrt{5}\times\sqrt{5}$ surface are shown in Figure 5. With a negative sample bias voltage, the adenine molecule (indicated by the white arrow) located adjacent to another molecule observed in Figure 5A moved by 70 Å from its original position after a scan performed with a large tunneling current $I = 700$ pA and $V_s = -2$ V, as shown in Figure 5B. The tip-assisted migration of the adenine molecule is also observed with a very low voltage $I = 70$ pA and $V_s = -0.02$ V, as shown in Figure 5C,D (indicated by the white arrow). Thus, molecule migration was observed in some different combinations of V_s and I, which seems to be uncorrelated. In contrast, with a positive sample voltage, the adenine molecules observed in Figure 5E disappeared from the surface after a high-voltage scan ($V_s = 4$ V and $I = 10$ pA), as shown in Figure 5F, suggesting the desorption of the adenine molecules. Therefore, the manipulation of adenine molecules exhibits significant polarity dependence, given the migration over the surface with a negative sample voltage and the desorption from the surface with a positive sample voltage.

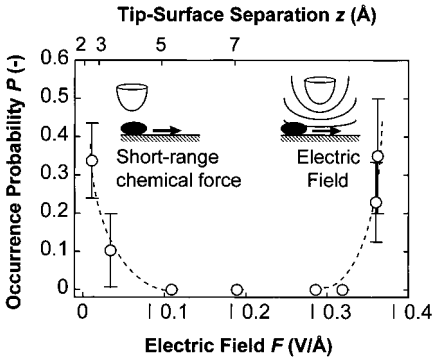

Figure 6. Variation of the probability P for tip-assisted migration as a function of manipulation field F, controlled using bias voltage V_s. The values of P are defined as the ratio of the number of molecules that have migrated to the total number of molecules. The thresholds are found at $F \cong -0.1$ V/Å and $F \cong -0.3$ V/Å.

To clarify the nature of tip−molecule interactions, the authors evaluated the occurrence probability P of tip-assisted migration and desorption as a function of voltage (V_s), current (I), tip−surface separation (z), and field ($F \approx V_s/z$). Direct evidence for voltage effect or current effect would exist in the complemental current dependence (fixed voltage) and voltage dependence (fixed current) of P. If the field effect or proximity effect were dominant, a threshold field or threshold tip−surface separation would appear on P regardless of V_s and I.

(c) Molecule Manipulation Induced by Tip Proximity. In this section, the authors investigated the probability of migration occurrence P for various negative sample voltages. The P values for migration are defined as the ratio of the number of molecules that have migrated to the number of total molecules. Figure 6 shows the P values for tip-assisted migration as a function of the electric field F obtained by the change of V_s ($V_s = -0.02$ to -5.0 V) with a fixed tunneling current $I \cong 10$ pA. This reveals two threshold fields for tip-assisted migration: below $F \cong -0.1$ V/Å and above $F \cong -0.3$ V/Å. The threshold at $F \cong -0.3$ V/Å corresponds to the increase of V_s from -4.0 to -5.0 V, suggesting the presence of an electric field effect on tip-assisted molecule migration. Details of this field effect are discussed along with tip-assisted desorption at positive sample voltage in the next section. This section, however, focuses on the tip-assisted migration, which occurs below the $F \cong -0.1$ V/Å threshold. The field below approximately -0.1 V/Å can be realized when V_s decreases from -0.1 to -0.02 V, and the tip closely approaches the surface for $z \cong 3$ Å ($z' \cong 4.4$ Å) (using the upper scale of Figure 6). This result means that lateral sliding would occur due to the atomic force if the magnitudes of I, V_s, and F become sufficiently small.

The atomic force comprises three different forces: long-range van der Waals attractive force, short-range chemical forces and repulsive force (physical contact). These forces can be adjusted by varying the separation between the tip and the adsorbate, to achieve precise pulling, sliding, and pushing processes.[32] In this case, $z' \cong 5.5$ Å (corresponding to tunneling resistance $R \cong 2$ GΩ), which is too great for the lateral pushing mechanism. In fact, the pushing mechanism has only been feasible for structurally high molecules such as Cu-TBP porphyrin,[1] C_{60},[2] and DNA oligomer,[3] whose structural height is more than approximately 8 Å. Since the height of adenine molecules is only 3−4 Å in the STM image shown in Figure 2, the short-range chemical force[27] between the tip and the molecule is expected to represent a possible mechanism. This short-range chemical force means a weak overlap of atomic orbitals (or potential curves) between a tip and adsorbed molecule. The

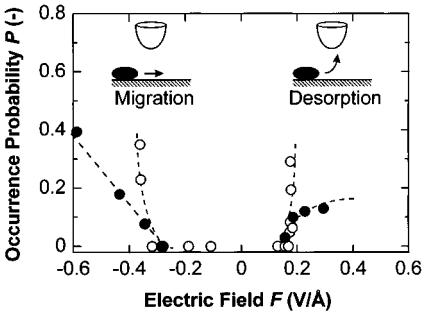

Figure 7. Variation of the probability P for tip-assisted migration and desorption as a function of manipulation field F. The values of P are defined as the ratio of the number of molecules that have migrated or desorbed to the number of total molecules. Hollow circles and solid circles represent the variations in bias voltage V_s for fixed tunneling current I, and variations in current I for fixed bias voltage V_s, respectively. The agreement of thresholds between the series of changes in V_s and I are found for each polarity, irrespective of different combinations of V_s and I.

authors could not specify what orbitals are concerned in this overlap because of the complication of tip condition; however, the π-orbital of adenine and the 5d-orbital of the Pt tip may be possible. The long-range van der Waals attractive force is too small to hold the molecule below the tip at room temperature.

(d) Electric Field Controlled Manipulation. Just as described in section 4c above, the authors evaluated the occurrence probability P for various values of V_s and I on tip-assisted migration and desorption. The P values were defined as the ratio of the number of molecules that have migrated or disappeared to the number of total molecules. Figure 7 shows the P values as a function of the electric field F. The plots involve some of the same data in Figure 6 (hollow circles above $F \cong -0.18$ V/Å). With a negative sample voltage, the value of P for migration rises above a threshold value of $F \cong -0.3$ V/Å as the current I increases from 70 to 7000 pA with a fixed bias of $V_s = -2.0$ V (left-hand solid circles). The value of P also rises at $F \cong -0.3$ V/Å as the voltage V_s increases from -4.0 to -5.0 V with a fixed current I of 7 pA (left-hand hollow circles). Despite the widely differing combinations of V_s and I, the threshold values of F observed in these two series agree well around $F \cong -0.3$ V/Å. This strongly suggests that the electric field F strongly influences the migration of adenine molecules.

Similarly, the values of P for desorption in a positive field agree closely with the thresholds of $F \cong -0.2$ V/Å for the series of changes in both voltage (right-hand hollow circle) and current (right-hand solid circle), irrespective of differences in the values of V_s and I at the threshold field. This implies that desorption is also strongly dependent on F. Accordingly, the following analysis and discussion focuses on the electrostatic influence at these threshold values of F on the migration and desorption of adenine molecules.

5. Mechanisms of Electric Field Controlled Manipulation

(a) Estimation of Molecule−Surface Charge Transfer. When the molecule was adsorbed on the surface, some charge transfer between the adsorbed molecule and the surface should occurred. This charge transfer can be described by the formation of a surface electric dipole moment, which consists of a monopole molecule charge and a counter monopole charge in the surface. The surface dipole moment forms an electric potential, which changes the effective surface work function for electron tunneling. Consequently, the authors measured the tunneling barrier-height images in order to estimate the mag-

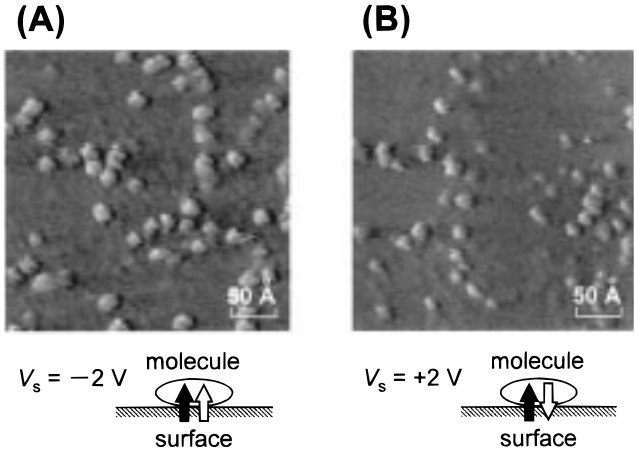

Figure 8. Barrier height images of adenine molecules adsorbed on an $SrTiO_3(100)$-$\sqrt{5}\times\sqrt{5}$ surface with (A) $V_s = -2$ V and (B) $V_s = 2$ V. In these images, the molecules always appear bright, suggesting that the barrier height is enhanced by the presence of adenine molecules. The insets show the directions of permanent dipole (black arrow) and induced dipole (white arrow).

nitude of the dipole moment on an adsorbed adenine molecule. The surface dipole moment can be expressed as

$$\mu = \Delta\Phi(\epsilon_0 S/e) \tag{3}$$

where $\Delta\Phi$ is the difference in the tunneling barrier height between the clean surface and the molecule-adsorbed surface.[33] S and ϵ_0 are the molecule size and the permittivity in free space, respectively. This expression implies that the tunneling electrons encounter a higher or lower barrier height than that of the clean surface when the electrons pass through an adsorbed molecule with an upward or downward dipole moment on the surfaces. As a result, the obtained value of μ possesses a permanent and induced dipole moment according to

$$\mu = \mu_p + \alpha F \tag{4}$$

where α is the polarizability and F is the electric field.[10−15]

The tunneling barrier-height images of the adenine molecules adsorbed on the $SrTiO_3(100)$-$\sqrt{5}\times\sqrt{5}$ surface at (A) $V_s = -2$ V and (B) $V_s = 2$ V are shown in Figure 8. The brighter points represent the higher tunneling barrier heights. In these observations, the molecules are always rendered brightly, which indicates that the barrier height is enhanced by the presence of the adenine molecules. This implies that the total dipole moment μ is always directed to the vacuum, despite the polarity change. The value of $\Delta\Phi$, however, changes with the value of F (see Figure 8 inset). In fact, the values of $\Delta\Phi$ obtained were 1.31 eV in (A) with $V_s = -2$ V and 0.93 eV in (B) with $V_s = 2$ V. This variation is attributed to the contribution of an induced dipole, for which the orientation is inverted by the polarity change of F. This result produces the values $\mu_p = -0.41 \times 10^{-29}$ C·m (1.23 D) and $\alpha = 0.65 \times 10^{-39}$ (C·m^2)/V (5.8 Å^3). Since the magnitude of μ_p is too large to attribute to an isolated adenine molecule, these results suggest that the adenine molecule has a negative charge that has been transferred from the $SrTiO_3$-(100)-$\sqrt{5}\times\sqrt{5}$ surface. The values are 0.21 electrons at $V_s = -2$ V and 0.15 electrons when the separation between surface and molecule r_0 is assumed to be 1.5 Å.

(b) Electric Dipole Effect on Surface Sliding and Field Evaporation. In general, the potential energy of a molecule in an electric field is given by

$$\Delta U = qV - \mu_p F - {}^1/_2\alpha F^2 \tag{5}$$

where q, μ_p, and α are the monopole charge, permanent dipole moment, and polarizability, respectively, and V is the electric potential.[10−15] As mentioned above, the authors found that the threshold for migration and desorption is solely dependent on electric field F. Accordingly, values of electric potential V in the first term of eq 5, which is given simply as the sample bias voltage V_s, do not significantly influence the mechanism of migration and desorption in this system. The contribution of electric field F to ΔU is made by the products of F and μ_p, and F^2 and α, in the second and third terms of eq 5, respectively. Accordingly, understanding the interaction between tip-field and dipole moments is essential to identify the manipulation mechanism involved.

The polarity dependence of the surface migration of the adenine molecule was considered first. Directional migration can be examined in terms of the potential difference of a molecule in a field, as shown in Figure 9 (inset). As mentioned above, the variation of potential energy ΔU is given by eq 5. The value of ΔU just below the tip as a function of F is represented in Figure 9 using the values of μ_p and α obtained above. The contribution of the permanent dipole moment (dashed line) and induced dipole moment (dotted line) shows a proportional and quadratic dependence on the electric field F, respectively. This implies that μ_p and αF are parallel for a negative field and antiparallel for a positive field, resulting in field-polarity asymmetry in terms of the ΔU curve for the total dipole moment (solid line). As a result, the value of $|\Delta U|$, which is a dominant factor affecting tip-assisted migration, has a greater effect for a negative field than a positive field. For example, the field threshold of $F = -0.3$ V/Å for tip-assisted migration shown in Figures 7 and 8 corresponds to $\Delta U = -0.1$ eV, as shown in Figure 9. The same absolute ΔU value for a negative threshold field cannot be achieved with a positive field, since ΔU is saturated below 0.08 eV at $F = -0.6$ V/Å, and achieving such a high value with a $SrTiO_3(100)$-$\sqrt{5}\times\sqrt{5}$ surface in a positive field is impractical, as shown in Figure 2. This strongly suggests that the induced dipole moment αF plays a decisive role in field-polarity dependence for tip-assisted migration.

Despite a small dipole effect occurring in a positive field, the remarkable phenomenon of tip-assisted desorption occurs in a low positive field. The dipole effect can also provide a deeper understanding of tip-assisted desorption, as illustrated by the following discussion based on field evaporation. The field evaporation is described as a transition from the neutral state to the ionic state, as shown in Figure 10A. The activation energy Q for this transition is reduced with increasing F because only the ionic state is inclined with an applied field F. Here, it should be noted that the value of Q also changes with the stability of an adenine molecule at the potential minimum neutral state, which is attributed to dipole effect $\Delta U(F)$. For a univalent cation, Q can be given by

$$Q^+_{(F)} = (\Lambda + I_1 - \Phi) - er_0F - \Delta U_{(F)} \tag{6}$$

where Λ is adsorption energy, I_1 is the ionization energy of the molecule, Φ is the work function of the clean surface, and r_0 is the stable adsorption radius.[8,10] When the terms $\Lambda + I_1 - \Phi$ are replaced by $\Lambda + \Phi - E_{aff}$, the value Q for a univalent anion is given by

$$Q(F) = (\Lambda + \Phi - E_{aff}) + er_0F - \Delta U_{(F)} \tag{7}$$

where E_{aff} is the electron affinity of the molecule.

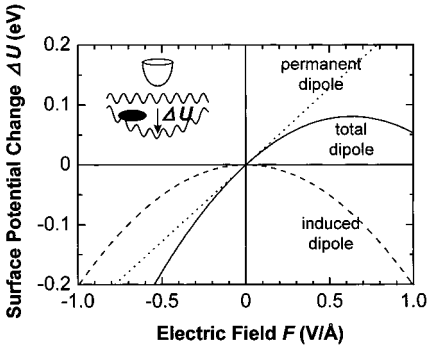

Figure 9. Variation in surface potential energy change ΔU just below the tip as a function of field F, and the schematic view of ΔU in the insets. The permanent dipole moment μ_p (dashed line) and the induced dipole moment αF (dotted line) are parallel for a negative field and nonparallel for a positive field, causing the ΔU curve to have field-polarity asymmetry in terms of the total dipole moment (solid line).

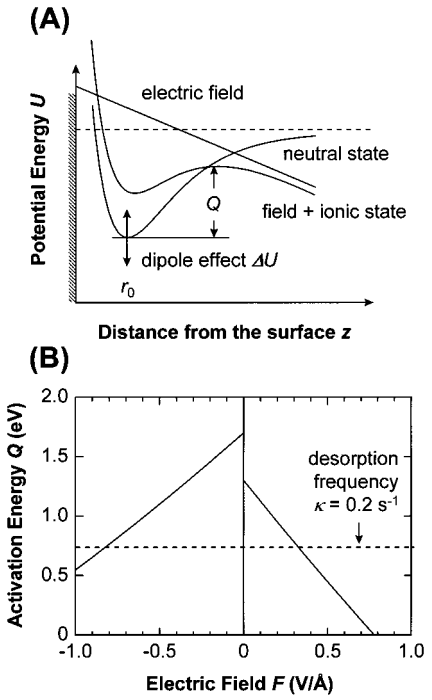

Figure 10. (A) Generally, field evaporation is described as a transition from a neutral state to an ionic state. The activation energy Q for this transition is reduced with increasing F because the inclination of the ionic state is only steep with an applied field. The value of Q also changes with the presence of the dipole moment yielded by ΔU. (B) Activation energy Q for the field evaporation of the univalent ion as a function of field F. The dotted line indicates the activation energy required to desorb the adsorbed molecule while the tip is passing over the molecule.

The Q curves were calculated as a function of F, as shown in Figure 10B. The values of Λ and r_0 were estimated to be $\Lambda = 1.5$ eV and $r_0 = 1.5$ Å, respectively, while the work function $\Phi = 4.2$ eV was obtained from photoemission spectroscopy data.[30] In general, the ionization energy of isolated molecules is significantly different from electron affinity, due to the large energy difference between the highest occupied molecular orbital (HOMO) and the lowest unoccupied molecular orbital (LUMO). For an isolated adenine molecule, a previous study and molecular orbital calculations have determined $I_1 \cong 8.5$ eV and $E_{aff} \cong 4.0$ eV.[34,35] The authors however, have assumed $I_1 = E_{aff} = 4.0$ eV for an adsorbed molecule on an $SrTiO_3(100)$-$\sqrt{5}\times\sqrt{5}$ surface, as the barrier-height measurement mentioned above shows the presence of a permanent dipole $\mu_p = -0.41 \times 10^{-29}$ C·m, suggesting that surface electrons are transferred to the LUMO of the adenine molecule. On the other hand, the dotted line indicates that $Q = 0.815$ eV, corresponding to a desorption frequency $\kappa = \nu \exp(-Q/kT) = 0.2\ s^{-1}$ at room temperature. This line indicates that the adsorbed molecule can desorb for as long as the tip passes over the molecule.

The points where the Q curve intersects this dotted line represent the threshold for field evaporation. For a positive field, the intersection point $F = 0.3$ V/Å correlates closely with the experimental value of $F = 0.2$ V/Å. In contrast, the intersection point for a negative field is $F = -0.8$ V/Å, which is impractically high for stable scanning and is much larger than the value of the negative intersection point. These results correlate closely with experimental data, suggesting that tip-assisted desorption occurs only for a positive field. In the Q curve calculation, the values for Λ and r_0 include a degree of uncertainty. The variation in Λ causes the energy shift, and r_0 determines the change in slope. However, since these variations affect both the positive and negative portions of the Q curve equally, these parameters do not alter the fact that the field evaporation threshold is lower for a positive field than a negative field.

This polarity difference of the threshold between the positive and negative fields is mainly due to the slope difference, which is determined by the permanent dipole moment μ_p. In this case, a positive field is favorable for field evaporation because of the resulting steep slope of the $Q^+_{(F)}$ curve. On the other hand, as shown in Figure 9, a negative field is effective for migration because $|\Delta U|$ is intensified by the induced dipole moment being parallel to the permanent dipole moment. This consideration shows that the polarity dependence of tip-assisted migration and desorption can be described by the electrostatic interaction of dipole moments using the simple model described here.

6. Conclusion

The authors have described three distinct manipulation modes for adenine molecules, which occur selectively depending upon the tip−surface separation, electric field, and the electric dipole moment of the molecules. Quantitative measurement of absolute tip−surface separation and electron tunneling barrier height permitted the contribution of proximity and electrostatic interactions to be estimated. On the basis of these measurements, the significant role of the dipole moment was revealed in field-induced sliding and evaporation. Furthermore, the close correspondence between experimental and calculated results was demonstrated, thus providing a general understanding of molecular manipulation. The authors believe that these results can be used to establish a methodology for the a priori design of molecular/surface systems for molecular manipulation.

References and Notes

(1) Jung, T. A.; et al. *Science* **1996**, *271*, 181.
(2) Gimzewski, J. K.; Modesti, S.; David, T.; Schlittler, R. R. *J. Vac. Sci. Technol.* **1994**, *B12*, 1942.
(3) Tanaka, H.; Kawai, T. *J. Vac. Sci. Technol. B* **1995**, *15*, 602.
(4) Forbes, R. G. *Appl. Surf. Sci.* **1995**, *87/88*, 1.
(5) Gomer, R.; Swanson, L. W. *J. Chem. Phys.* **1963**, *38*, 1613.
(6) Lyo, I. W.; Avouris, P. *Science* **1991**, *253*, 173.
(7) Hosoki, S.; Hosaka, S.; Hasegawa, T. *Appl. Surf. Sci.* **1992**, *60/61*, 643.
(8) Tsong, T. T. *Phys. Rev. B* **1991**, *44*, 13703.
(9) Eigler, D. M.; Lutz, C. P.; Rudge, W. E. *Nature* **1991**, *352*, 600.
(10) Tsong, T. T.; Chang, C. S. *Jpn. J. Appl. Phys.* **1995**, *34*, 3309.
(11) Akiyama, R.; Matsumoto, T.; Kawai, T. *Appl. Phys. A* **1998**, *66*, S719.
(12) Akiyama, R.; Matsumoto, T.; Kawai, T. *Surf. Sci. Lett.* **1998**, *418*, L73.

(13) Stroscio, J. A.; Eigler, D. M. *Science* **1991**, *254*, 1319.
(14) Nakayama, T.; Aono, M. In *Proc. Sci. Technol. Atom. Eng. Mater. 99*; Jena, P., Khanna, S. N., Rao, B. K., Eds., World Scientific: Singapore, 1996.
(15) Whitman, L. J.; Stroscio, J. A.; Dragoset, R. A.; Celotta, R. J. *Science* **1991**, *251*, 1206.
(16) Shen, T. C.; et al. *Science* **1995**, *268*, 1590.
(17) Avouris, Ph.; et al. *Surf. Sci.* **1996**, *363*, 368.
(18) Tanaka, H.; Nakagawa, T.; Kawai, T. *Surf. Sci.* **1996**, *364*, L575.
(19) Kasaya, M.; Tabata, H.; Kawai, T. *Surf. Sci.* **1995**, *342*, 215.
(20) Kasaya, M.; Tabata, H.; Kawai, T. *Surf. Sci.* **1996**, *357/358*, 195.
(21) Tanaka, H.; Kawai, T. *J. Vac. Sci. Technol. B* **1995**, *13*, 1411.
(22) Tanaka, H.; Kawai, T. *Mater. Sci. Eng. C* **1995**, *3*, 143.
(23) Tanaka, H.; Matsumoto, T.; Kawai T.; Kawai, S. *Jpn. J. Appl. Phys.* **1993**, *32*, 1405.
(24) Yazdani, A.; Eigler, D. M.; Lang, N. D. *Science* **1996**, *272*, 1921.
(25) Gimzewski, J. K.; Moller, R. *Phys. Rev. B* **1987**, *36*, 1284.
(26) Chen, C. J.; Hammers, R. J. *J. Vac. Sci. Technol. B* **1991**, *9*, 503.
(27) Olesen, L.; Brandbyge, M.; Sorensen, M. R.; Jacobsen, K. W.; Lagsgaard, E.; Besenbacher F. *Phys. Rev. Lett.* **1993**, *76*, 1485.
(28) Olesen, L.; Lagsgaard, E.; Stensgaard, I.; Besenbacher, F. *Appl. Phys. A* **1998**, *66*, S157.
(29) Abraham, D. W.; Mamin, H. J.; Ganz, E.; Clarke, J. *IBM J. Res. Dev.* **1986**, *30*, 492.
(30) Private communication with Y. Aiura of the National Institute of Electrotechnical Laboratory.
(31) Akiyama, R.; Matsumoto, T.; Tanaka, H.; Kawai, T. *Jpn. J. Appl. Phys.* **1997**, *36*, 3881.
(32) Meyer, G.; Rieder, K. H. *MRS Bull.* **1998**, Jan., 28.
(33) Spong, J. K.; et al. *Nature* **1989**, *338*, 137.
(34) Xi, M.; Yang, M. X.; Jo, S. K.; Bent, B. E. *J. Chem. Phys.* **1994**, *101*, 9122.
(35) Urano, S.; Yang, X.; Lebreton, P. R. *J. Mol. Struct.* **1989**, *214*, 315.